Available online at www.sciencedirect.com
ScienceDirect
Journal of the European Ceramic Society 27 (2007) 2989–2993
www.elsevier.com/locate/jeurceramsoc

Relationship between crystal structure and microwave dielectric properties of melilite-type ceramic

Atsushi Yokoi *, Hirotaka Ogawa, Akinori Kan, Yoshifumi Nakamura

Faculty of Science and Technology, Meijo University, 1-501 Shiogamaguchi, Tenpaku-ku, Nagoya 468-8502, Japan

Abstract

Crystal structure–microwave dielectric property relations in the melilite-type $Ba_2(Mg_{1-x}Zn_x)Si_2O_7$ ceramics were investigated in this study. The formation of a secondary phase was not detected over the whole composition range. Also, the lattice parameter, a, of the solid solutions decreased linearly with increasing the composition x, while the lattice parameter, c, was increased by the Zn substitution for Mg. Also, the covalency of the Mg—O bond increased from 26 to 35% in the composition range of 0–0.75. Moreover, the covalency of the Zn—O bond increased in the composition range of 0.25–1, while that of Si—O bonds in the SiO_4 tetrahedron remained approximately constant over the whole composition range. The dielectric constants (ε_r) of the solid solutions were on the order of approximately 7.5, and the quality factors ($Q{\cdot}f$) of the solid solutions increased with increasing the composition x. The temperature coefficient of resonant frequency (τ_f) of the solid solutions varied from −62 to −74 ppm/°C with increasing the composition x; therefore, the Zn substitution for Mg was not effective in improving the τ_f value in this system.

Keywords: Sintering; Dielectric properties; Microwave dielectrics

1. Introduction

In the commercial applications such as the high-frequency systems, the silicates have been reported as the attractive candidates for use.[1] A low dielectric constant (ε_r), a high quality factor ($Q{\cdot}f$) and a near zero temperature coefficient of resonant frequency (τ_f) are generally required for these applications.[2] The forsterite (Mg_2SiO_4) ceramic is well known to have the microwave dielectric properties: $\varepsilon_r = 7.8$, $Q{\cdot}f = 240{,}000$ GHz and $\tau_f = -67$ ppm/°C.[3] However, the continuous development of wireless communication technology will rely upon the identification of new dielectric ceramics with the appropriate microwave dielectric properties as described above.

In recent work, it has been reported that the several mixed alkaline earth and transition metal silicates, which have the melilite-type crystal structure with space group of $C12/c1$ (no. 15), are represented as $M_2M'Si_2O_7$, where M is an alkaline earth and M′ is a transition metal.[4,5] However, the microwave dielectric properties of these compounds have not been reported to date. Thus, in order to clarify the microwave dielectric properties of $Ba_2MgSi_2O_7$ ceramic, the $Ba_2MgSi_2O_7$ ceramic was synthesized, the Zn substitution for Mg was performed, and the crystal structure–microwave dielectric property relationship of the $Ba_2(Mg_{1-x}Zn_x)Si_2O_7$ solid solutions were investigated in this study.

2. Experimental method

High-purity (>99.9%) $BaCO_3$, MgO, ZnO and SiO_2 powders weighed on the basis of the their stoichiometric composition were mixed and calcined at 1000 °C for 10 h in air. These calcined powders were milled and mixed with a polyvinyl alcohol, and then pressed into a pellet of 12 mm in diameter and 7 mm in thickness under the pressure of 100 MPa. Subsequently, these pellets were sintered at the various temperatures ranging from 1300 to 1350 °C for 10 h in air. The crystalline phases were identified by X-ray powder diffraction (XRPD). The lattice parameters and the crystal structures of the samples were refined by using Rietveld analysis (RIETAN).[6,7] The dielectric constants and the quality factors were measured by the Hakki–Coleman method.[8] The τ_f values were determined from the differences in the resonant frequencies obtained at the temperatures of 20 and 80 °C.

* Corresponding author. Tel.: +81 52 832 1151x5160; fax: +81 52 832 1253.
E-mail address: ogawah@ccmfs.meijo-u.ac.jp (A. Yokoi).

0955-2219/$ – see front matter © 2006 Elsevier Ltd. All rights reserved.
doi:10.1016/j.jeurceramsoc.2006.11.069

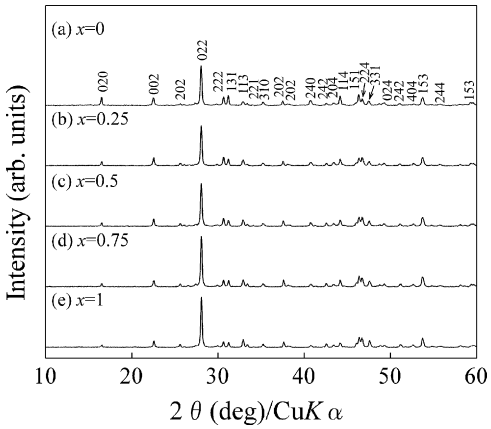

Fig. 1. XRPD patterns of $Ba_2(Mg_{1-x}Zn_x)Si_2O_7$ solid solutions sintered at various temperatures for 10 h in air.

3. Results and discussion

Fig. 1 shows the XRPD patterns of $Ba_2(Mg_{1-x}Zn_x)Si_2O_7$ solid solutions sintered at various temperatures for 10 h in air. From the XRPD results of Zn-substituted $Ba_2(Mg_{1-x}Zn_x)Si_2O_7$ solid solutions, the samples over the whole composition range showed a single phase, which was a monoclinic crystal structure with $C12/c1$ space group. In the crystal structure of $Ba_2MgSi_2O_7$ ceramic, the crystal structure consists of MgO_4 tetrahedron which share their oxygen atoms with those of the $[Si_2O_7]^{6-}$, and the two-dimensional extended layers are separated by the Ba atoms, as shown in Fig. 2. Moreover, the peak shifts to smaller angle of 2θ are recognized with increasing the composition x as shown in Fig. 1. Thus, it was expected that the lattice parameters and the unit cell volume were varied by the Zn substitution for Mg; therefore, the lattice parameters and the unit cell volume of the $Ba_2(Mg_{1-x}Zn_x)Si_2O_7$ solid solutions were refined in terms of the Rietveld analysis, and the results are shown in Fig. 3. A linear dependence of the lattice parameters in the solid solutions was observed; the lattice parameter, a, decreased linearly with increasing the composition x, while the lattice parameter, c, was increased by the Zn substitution for Mg. Furthermore, no variations in the lattice parameter, b, of the solid solutions was observed in the composition range of 0–1. From the results of these variations in the lattice parameters, the $Ba_2(Mg_{1-x}Zn_x)Si_2O_7$ solid solutions satisfy Vegard's low which confirms the formation of the solid solutions because all the lattice parameters vary linearly throughout the entire composition range. Also, the unit cell volume of the solids solutions was on the order of approximately 713.5 $Å^3$, because the variation in the lattice parameter, a, was symmetric with respect to that in the lattice parameter, b, caused by the Zn substitution for Mg. As mentioned previously, the crystal structure of $Ba_2(Mg_{1-x}Zn_x)Si_2O_7$ solid solutions is composed of the (Mg, Zn)O_4 and SiO_4 tetrahedra as shown in Fig. 4.

The effects of Zn substitution for Mg on the volumes of these tetrahedra in the $Ba_2(Mg_{1-x}Zn_x)Si_2O_7$ solid solutions are shown in Fig. 5. Although any remarkable variations in the volume of the SiO_4 tetrahedra were not observed in the composition range of 0–1, the volume in the (Mg, Zn)O_4 tetrahedra

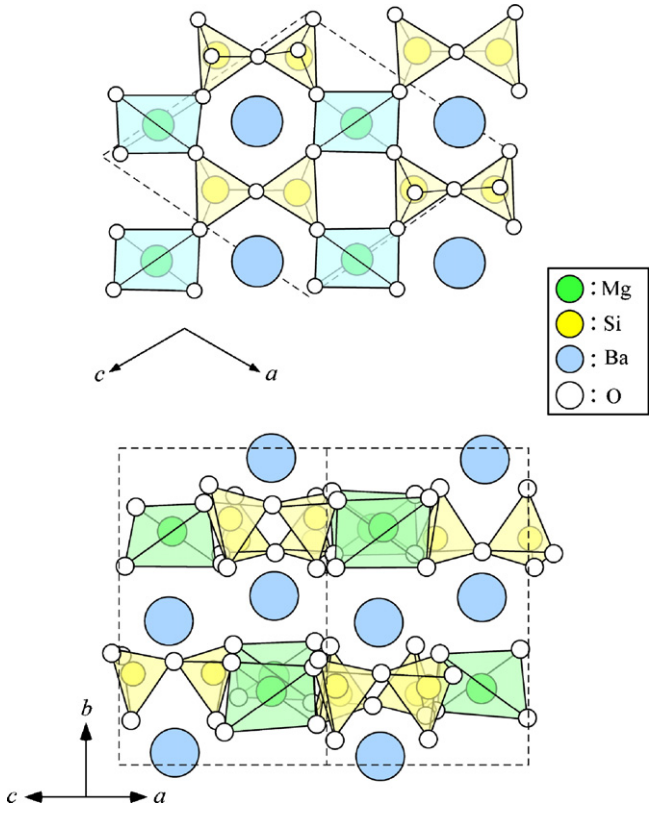

Fig. 2. Schematic diagram of crystal structure of melilite-type $Ba_2MgSi_2O_7$ ceramic.

in the $Ba_2(Mg_{1-x}Zn_x)Si_2O_7$ solid solutions was observed to be linear, depending on the composition x; that of the (Mg, Zn)O_4 tetrahedra decreased. Thus, the unit cell volume of the $Ba_2(Mg_{1-x}Zn_x)Si_2O_7$ solid solutions is independent of the variations in the (Mg, Zn)O_4 tetrahedra caused by the Zn substitution for Mg. It is also considered that the variations in the atomic distance in the (Mg, Zn)O_4 and MgO_4 tetrahedra caused by the Zn substitution for Mg are associated with the volume of these tetrahedra. Thus, in order to clarify the variations in the atomic distances of (Mg, Zn)O_4 and MgO_4 tetrahedra, they were investigated in this study. In the (Mg, Zn)O_4 tetrahedra, the decreases in oxygen–oxygen distances such as O(2)–O(3′), O(2′)–O(3), O(2)–O(2′) and O(3)–O(3′) bonds were observed with the Zn substitution for Mg. Since the direction of the O(2′)–O(3) bond in the (Mg, Zn)O_4 tetrahedra are parallel to that of the a-axis, it is considered that the increase in the lattice parameter, a, as shown in Fig. 3 relates closely with the variations in the atomic distances of the O(2′)–O(3) bond.

As for the SiO_4 tetrahedron, the increases in Si–oxygen distance such as the Si–O(4) bond and in oxygen–oxygen distances such as the O(1)–O(3), O(2)–O(4) and O(3)–O(4) bonds were recognized with the Zn substitution for Mg. Furthermore, we focus on the bond angle of Si–O(4)–Si in the $[Si_2O_7]^{2-}$ group; therefore, the bond angle of Si–O(4)–Si in the $[Si_2O_7]^{6-}$ group, which were calculated from the results of the Rietveld analysis, are shown in Fig. 6. The bond angle of Si–O(4)–Si of the $Ba_2MgSi_2O_7$ ceramic was approximately 147.5° and the value of the $Ba_2MgSi_2O_7$ ceramic was consistent with several

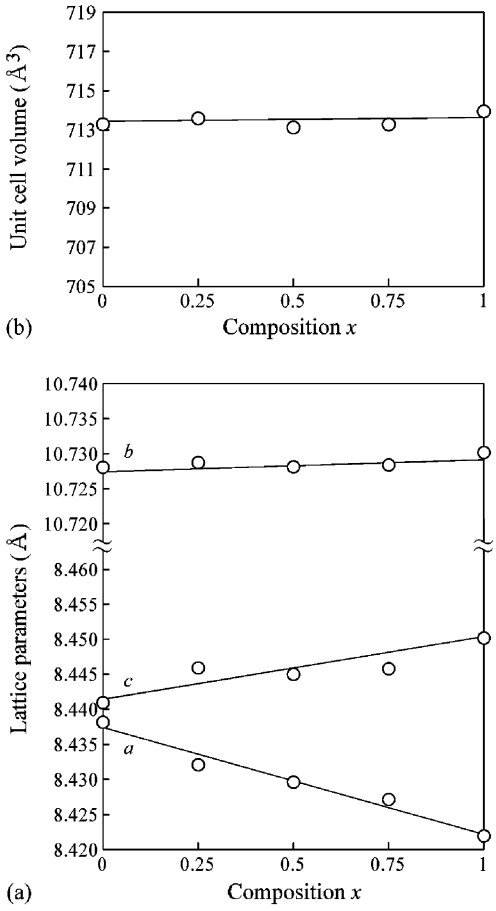

Fig. 3. Variations in (a) lattice parameters and (b) unit cell volume of $Ba_2(Mg_{1-x}Zn_x)Si_2O_7$ solid solutions as a function of composition x.

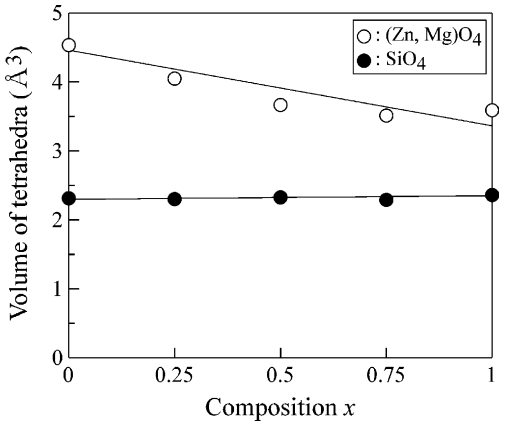

Fig. 5. Effect of Zn substitution for Mg on volume of (Mg, Zn)O_4 and SiO_4 tetrahedra as a function of composition x.

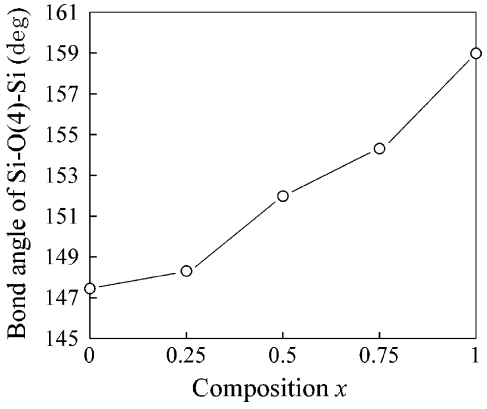

Fig. 6. Variation in bond angle of Si–O(4)–Si in $[Si_2O_7]^{6-}$ group as a function of composition x.

of the silicates.[9] Moreover, the bond angle of Si–O(4)–Si of the $Ba_2(Mg_{1-x}Zn_x)Si_2O_7$ solid solutions increased linearly from 147.5° to 159°, depending on the composition x. Therefore, it is recognized that the bond angle of Si–O(4)–Si in the $[Si_2O_7]^{6-}$ group approaches the bond angle of 180° with increasing the composition x.

Although the volume and the atomic distances of (Mg, Zn)O_4 and SiO_4 tetrahedra, and the bond angle of Si–O(4)–Si in the $[Si_2O_7]^{2-}$ group were clarified, the effects of Zn substitution for Mg on the covalency of cation–oxygen bonds have not been investigated; it is expected that these variations in the covalency of cation–oxygen bonds exert an influence on the microwave dielectric properties.[10] Therefore, the covalencies of cation–oxygen bonds over the whole composition range were calculated by using the refined bond length. The relationship between the covalency and the bond length is given by two equations[11–13]:

$$s = \left(\frac{R}{R_1}\right)^{-N} \tag{1}$$

and

$$f_c' = \mathrm{as}^M \tag{2}$$

where s is the bond strength, R the refined bond length and R_1, N, a and M are the empirically determined parameters, which were reported by Brown et al.[12,13] The covalencies of Zn–O, Mg–O and Si–O bonds in the (Mg, Zn)O_4 and SiO_4 tetrahedra

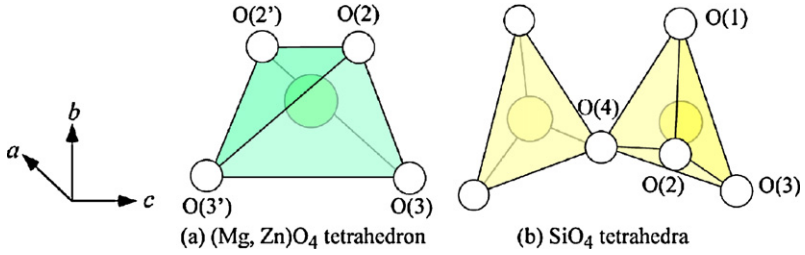

Fig. 4. Schematic representations of (Mg, Zn)O_4 and SiO_4 tetrahedra.

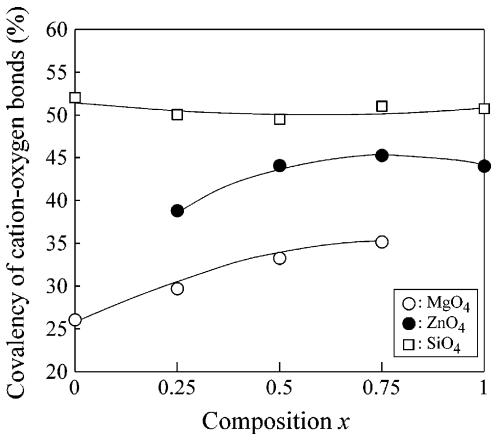

Fig. 7. Effects of Zn substitution for Mg on covalency of cation–oxygen bonds as a function of composition x.

caused by the Zn substitution for Mg are shown in Fig. 7. In the case of the MgO_4 tetrahedron, the covalency of the Mg–O bond increased from 26 to 35% in the composition range of 0–0.75. Thus, the increase in the covalency of the Mg–O bond in the MgO_4 tetrahedron is due to the decrease in the bond length of Mg–O(3) and Mg–O(3′) bonds caused by the Zn substitution for Mg. The covalency of the Zn–O bond increased in the composition range of 0.25–1, while the covalency of Si–O bonds in the SiO_4 tetrahedron was on the order of approximately 50% over the whole composition range. From these results, it is suggested that the Zn substitution for Mg primarily exerts an influence on the covalency of Mg–O and Zn–O bonds in the (Mg, Zn)O_4 tetrahedra. Also, the increase in the covalency of Mg–O and Zn–O bonds in the (Mg, Zn)O_4 tetrahedra may be attributed to the variation in the bond angle of Si–O(4)–Si in the $[Si_2O_7]^{6-}$ group caused by the Zn substitution for Mg, because the (Mg, Zn)O_4 tetrahedra and $[Si_2O_7]^{6-}$ group are composed of shared oxygen atoms. Moreover, the average total covalency of Mg–O, Zn–O and Si–O bonds of the $Ba_2(Mg_{1-x}Zn_x)Si_2O_7$ solid solutions is shown in Fig. 8. The average total covalency of these bonds remained the constant value of approximately 46% in the composition range of 0–1. Thus, the variations in the average total covalency of the Mg–O, Zn–O and Si–O bonds of the $Ba_2(Mg_{1-x}Zn_x)Si_2O_7$ solid solutions may be associated with the

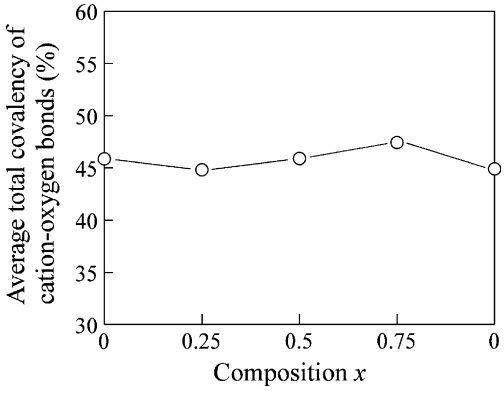

Fig. 8. Variation in average total covalency of Mg–O, Zn–O and Si–O bonds as a function of composition x.

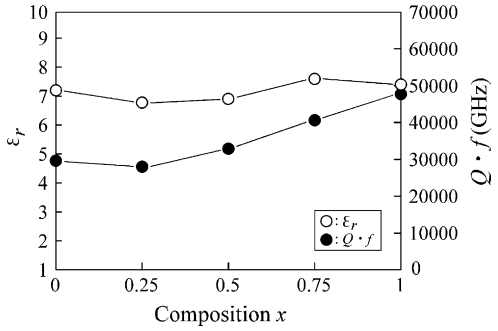

Fig. 9. Variations in ε_r and $Q{\cdot}f$ values of $Ba_2(Mg_{1-x}Zn_x)Si_2O_7$ solid solutions as a function of composition x.

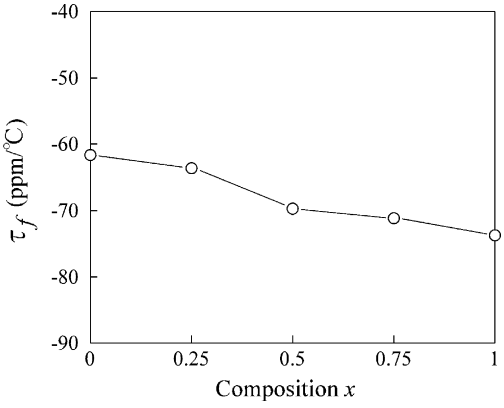

Fig. 10. Temperature dependence of dielectric constant of $Ba_2(Mg_{1-x}Zn_x)Si_2O_7$ solid solutions as a function of composition x.

microwave dielectric properties caused by the Zn substitution for Mg.

The microwave dielectric properties of $Ba_2(Mg_{1-x}Zn_x)Si_2O_7$ solid solutions are shown in Figs. 9 and 10. The ε_r values of the solid solutions are on the order of approximately 7.5 in the composition range of 0–1; therefore, the variation in the ε_r values may be correlated with the average total covalency of cation–oxygen bonds caused by the Zn substitution for Mg, because the ε_r and the average total covalency shows a similar tendency in the composition range of 0–1. Moreover, the $Q{\cdot}f$ values of the solid solutions increased linearly from approximately 30,000 to 48,000 GHz, depending on the composition x. Thus, the highest $Q{\cdot}f$ value of 48,000 GHz was obtained at $x = 1$, and the Zn substitution for Mg was effective in improving the $Q{\cdot}f$ values in this system. The τ_f value of the solid solutions varied from −62 to −74 ppm/°C with increasing the composition x; therefore, the substitution of the other elements in this system is necessary in order to improve the τ_f value.

4. Conclusion

The $Ba_2(Mg_{1-x}Zn_x)Si_2O_7$ solid solutions were prepared and the relationship between the crystal structure and the microwave dielectric properties were investigated in this study. From the Rietveld analysis, it was found that the Zn substitution for Mg in $Ba_2(Mg_{1-x}Zn_x)Si_2O_7$ solid solutions showed a single phase of melilite-type structure over the whole composition range.

The bond angle of Si–O(4)O–Si in the $[Si_2O_7]^{2-}$ group were increased by the Zn substitution for Mg. The covalency of the Mg–O bond in the MgO_4 tetrahedra increased from 26 to 35% in the composition range of 0–0.75, and that of Zn–O bond in the ZnO_4 tetrahedra also increased in the composition range of 0.25–1. On the other hand, the covalency of the Si–O bond in the SiO_4 tetrahedron remained the constant value of approximately 50% over the whole composition range. From the results of the covalency of cation–oxygen bonds in the (Mg, Zn)O_4 and SiO_4 tetrahedra, the average total covalency of cation–oxygen bonds in the (Mg, Zn)O_4 and SiO_4 tetrahedra remain unaltered over the whole composition range. The dielectric constants of the solid solutions are on the order of approximately 7.5; therefore, the dielectric constant of the solid solutions may be attributed to the average total covalency of Mg–O, Zn–O and Si–O bonds of the $Ba_2(Mg_{1-x}Zn_x)Si_2O_7$ solid solutions. Moreover, the $Q{\cdot}f$ values of the solid solutions are increased by the Zn substitution for Mg; therefore, it is recognized that the Zn substitution for Mg is effective in improving the $Q{\cdot}f$ value in this system. The τ_f values of the solid solutions in the composition range of 0–1 vary from −62 to −74 ppm/°C; therefore, the substitution of the other elements in this system is necessary in order to improve the τ_f values.

References

1. Ohsato, H., Research and development of microwave dielectric ceramics for wireless communications. *J. Ceram. Soc. Jpn.*, 2005, **113**, 703–711.
2. Sugiyama, T., Tsunooka, T., Kakimoto, K. and Ohsato, H., Microwave dielectric properties of forsterite-based solid solutions. *J. Eur. Ceram. Soc.*, 2006, **26**, 2097–2100.
3. Ohsato, H., Tsunooka, T., Ando, M., Ohichi, Y., Miyauchi, Y. and Kakimoto, K., Millimeter-wave dielectric ceramics of almina and forsterite with high quality factor and low dielectric constant. *J. Korean Ceram. Soc.*, 2003, **40**, 350–353.
4. Richard, D. A., Ralph, L., Christophe, P. and Timir, D., Syntheses, structural analyses, and unusual magnetic properties of $Ba_2CoSi_2O_7$ and $BaCo_2Si_2O_7$. *Inorg. Chem.*, 1996, **35**, 3492–3497.
5. Tamura, T., Yoshiasa, A., Ishii, K., Takeno, S., Maeda, H., Emura, S. *et al.*, Local structure of $(Ca,Sr)_2(Mg,Co,Zn)Si_2O_7$ melilite solid-solution with modulated structure. *Phys. Chem. Miner.*, 1996, **23**, 81–88.
6. Rietveld, H. M., Profile refinement method for nuclear and metal urinates. *J. Appl. Crystallogr.*, 1969, **2**, 65–71.
7. Izumi, F., In *Rierveld Method*, ed. R. Young. Oxford University Press, Oxford, 1993 [chapter 13].
8. Hakki, B. W. and Coleman, P. D., A dielectric resonator method of measuring inductive in the millimeter range. *IRE Trans. Microw. Theory Technol.*, 1960, **MTT-8**, 402–410.
9. Plaisier, R. D., Jansen, J., G. de Graaff, R. A. and Ijdo, D. J. W., Structure determination of $Ca_3HfSi_2O_9$ and $Ca_3ZnSi_2O_9$ from powder diffraction. *J. Solid State Chem.*, 1995, **115**, 464–468.
10. Kan, A., Ogawa, H., Mori, K., Ohsato, H. and Ando, Y., Chemical bonding characteristics and dielectric properties of $Nd_2(Ba_{1-x}Sr_x)ZnO_5$ solid solutions. *J. Mater. Res.*, 2003, **18**, 2427–2434.
11. Brese, N. E. and O'Keeffe, M., Bond-valence parameters for solids. *Acta Cryst. B*, 1991, **47**, 192–197.
12. Brown, I. D. and Shannon, R. D., Empirical bond-strength-bond-length curves for oxides. *Acta Cryst. A*, 1973, **29**, 266–282.
13. Brown, I. D. and Wu, K. K., Empirical parameters for calculating cation–oxygen bond valences. *Acta Cryst. B*, 1976, **32**, 1957–1959.